INTERNATIONAL JOURNAL OF CLIMATOLOGY
*Int. J. Climatol.* (in press)
Published online in Wiley InterScience
(www.interscience.wiley.com) DOI: 10.1002/joc.1459

RMetS
ROYAL METEOROLOGICAL SOCIETY

# A regional high-frequency reconstruction of May–June precipitation in the north Aegean from oak tree rings, A.D. 1089–1989

Carol Griggs[a,*] Arthur DeGaetano,[b] Peter Kuniholm[a] and Maryanne Newton[a]
[a] *Cornell University, Malcolm and Carolyn Wiener Laboratory for Aegean and Near Eastern Dendrochronology, New York*
[b] *Cornell University, Earth and Atmospheric Sciences, New York*

## Abstract:

May–June precipitation is the primary limiting factor in annual tree-ring growth of the oaks of northeastern Greece and northwestern Turkey (39–42 N, 22–37 E). In a regional tree-ring chronology of historic building and modern forest samples, the May–June precipitation explains at least 40% of the variance for 1900–1985, and is reconstructed here from A.D. 1089–1989. The reconstruction is compared to three other precipitation reconstructions for Turkey. The mean temperature of May and June is also a growth-limiting factor owing to its effect on the availability of precipitation to the trees, but is more difficult to calibrate and reconstruct accurately owing to the trees' indirect response and the low number of long-temperature records available for the interior of northwestern Turkey.

An analysis of the various methods of manipulating oak tree-ring data for regional climate reconstruction shows that removing all but the high-frequency variability plus normalizing the oak data sets before combining them into a master chronology are optimal techniques for a reasonable precipitation reconstruction of the entire area over the instrumental period. However, these methods do remove the low-frequency signal and dampen some of the evidence of local extremes in May–June precipitation; these issues are discussed here and will be addressed in future research. 

KEY WORDS dendrochronology; regional dendroclimatology; oak tree-ring chronology; *Quercus* spp.; May–June precipitation reconstruction; north Aegean; NE Greece; NW Turkey

*Received 2 October 2006; Accepted 21 October 2006*

## INTRODUCTION

The common signal recorded in tree-ring patterns from Turkey, Greece, and surrounding countries is the basis for dating wood from historical and archaeological sites at the Malcolm and Carolyn Wiener Laboratory for Aegean and Near Eastern Dendrochronology at Cornell University. Analyses of an oak tree-ring chronology of forests and historic sites covering most of the second millennium A.D. for northeastern Greece and northwestern Turkey indicate that the primary growth-limiting climate factor recorded in their common signal is the total precipitation of May and June, the period in which most of the growing-season rainfall occurs in the region.

The high-resolution accuracy of the climate signal in tree rings is unique owing to the annual record of tree rings, replication of that record, and the record's ability to be securely dated to calendar years. This study focuses on the high resolution of the tree-ring record on a regional scale. Many years that have been labeled as extremes by historic records and/or single site or smaller area chronologies are dampened in this chronology since the region is about 1800 km in longitude. In the reconstruction, the extreme values indicate only years when an extreme is consistent over most of the region or very extreme in a small part of the region.

The low-frequency record in tree-ring widths is problematic due to several variables. One variable is the method of removing the nonclimatic response from the tree-ring measurements. While care is taken in choosing a curve for detrending (removing the growth trend due to a tree's age and other nonclimatic factors), climate response in the patterns can be unwittingly removed, and nonclimatic factors retained (Fritts, 1976; Cook and Kairiukstis, 1990). Combining multiple samples dampens noise that was not removed by detrending, but whether the climate response is accurately preserved despite possible removal from one or more of the samples is a persistent question. Detrending by conservative curves is one accepted solution, and comparing the results of detrending by different methods can indicate possible problems.

Detrending also approximately equalizes the average of each sample's ring widths, a reason that chronologies

*Correspondence to: Carol Griggs, Cornell University, Malcolm and Carolyn Wiener Laboratory for Aegean and Near Eastern Dendrochronology, New York. E-mail: cbg4@cornell.edu

contain only an accurate record of low-frequency patterns whose lengths are less than half the average sample length. The addition and subtraction of samples over time also makes the 'segment length curse' applicable in attempting spectral analysis (Cook *et al*., 1995).

In our chronology, the May–June precipitation accounts for at least 40% of the variance and only annual to subdecadal changes in May–June rainfall are reconstructed. There are many other factors, such as temperature, precipitation outside of May–June, and variations in the length of the growing season, that contribute to ring growth. For these reasons, the results are a rather flat record for 900 years. We compare the similarities and differences of the reconstruction to the regional low-frequency patterns in the tree rings in the discussion, and the nature of the low-frequency patterns is under current investigation (Griggs *et al*., 2005; Griggs, 2006).

The availability of the limited precipitation to the trees in this region is critical to the oaks' cambial activity (Kramer and Kozlowski, 1979) and thus to the complete range of their annual ring widths. The oaks are growing at the southern edge of a subhumid mesothermic climate regime, bordering the Mediterranean regime to the south (Zohary, 1973; Xoplaki, 2002), and the boundary is also approximately the southern boundary of the geographic ranges of the included forest species: *Quercus frainetto* Ten., *Q. hartwissiana* Steven, *Q. petraea* (Mattuschka) Liebl., and *Q. robur* L. (Davis, 1982). The blue oaks (*Q. douglasii* Hook. and Arn.) of west-central California, a region with a similar climate to the north Aegean, are equally sensitive to precipitation (Stahle *et al*., 2001), as are the post oaks (*Q. stallata* Wangenh.) in the south-central United States, where the geographic location of the prairie-forest border is caused by the amount of annual precipitation (Stahle and Hehr, 1984). White oaks (*Quercus alba* L.) in the central and eastern United States respond to annual precipitation in drought years, but with a limited response in wet years (Cook and Jacoby, 1979; Duvick and Blasing, 1981; Blasing and Duvick, 1984). European oak tree-ring chronologies have been analyzed for possible climate signals over much of the temperate species' ranges, but the oaks' growth response to limiting climate factors has been difficult to quantify (Baillie, 1982, 1995; Kelly *et al*., 2002; Wilson and Elling, 2004; García-Suárez, 2005).

The use of historical and archaeological tree-ring data as paleoclimate proxy data is currently under scrutiny here and in other regions (Kelly *et al*., 2002; Wilson *et al*., 2004). Two critical issues are that the samples were collected for a nondendroclimatic purpose, and that there is generally no record of the original source of the timber. The location of each sample on its parent tree, including compass direction and height on the bole, plus each tree's immediate environment are impossible to discern for the historic sites' timbers, and only to a limited degree in the forest sites where we often collect from stacks of freshly logged timber. However, we believe that the secure crossdating of the samples, both within and between sites, the number of samples, and the large area of the study region offset both issues and justify the use of our oak chronology as proxy data (Fritts, 1976; Cook and Kairiukstis, 1990).

Previous research using modern oak, pine, juniper, and cedar chronologies in the Mediterranean region has shown that wide *versus* narrow rings correspond to signature years of high *versus* low precipitation (Gassner and Christiansen-Weniger, 1942), and that signature growth years correspond to persistent anomalies in atmospheric circulation patterns (Hughes *et al*., 2001). March–June precipitation has been reconstructed from a single site oak chronology in the north-central region of Turkey, 1635–2000 (Akkemik *et al*., 2005); February–June precipitation has been reconstructed for Sivas, Turkey, 1628–1980 from chronologies of five different species from around Turkey including the one used here (D'Arrigo and Cullen, 2001); and May–June precipitation has been reconstructed for 1323–1998 from juniper and for 1776–1998 from juniper, pine, and cedar, all from sites in southwestern Turkey (Touchan *et al*., 2003). Their reconstructions are compared to ours in the Results and Discussion section.

## THE REGION

### *Geography and climate*

The area of northeastern Greece and northwestern Turkey (39–42 N, 22–37 E) was selected as the study region from the locations of seven sampled oak forest sites and the high number of oak samples collected from many buildings in that region (Figure 1, Table I). The area was subdivided into three grids from east to west. The western grid is composed of the Thessaloniki-Larisa area east of the Pindus Mountains and extending eastward along the north side of the Aegean Sea (Grid 1 at 22–26 E); the center grid includes the east Aegean and Marmara Sea transition regions, a more coastal environment (Grid 2 at 26–32 E); and the eastern grid is composed of the interior of the Black Sea ecoregion plus a small part of inner Anatolia (Grid 3 at 32–37 E) (Atalay, 2002; Xoplaki, 2002). The entire area has very low summer precipitation and during the rest of the year has fairly constant precipitation in the two outer grids with the highest variation in the center grid where the winter months have the highest precipitation.

The May–June average precipitation ranges from 56 to 136 mm (average 84 mm), with an increase from west to east. The average values are smaller than the May–June precipitation immediately along the Black Sea coast (67–230 mm, average 108 mm) and higher than that along the Mediterranean coast (27–66 mm, average 49 mm).

## DATA AND METHODS

### *Tree-ring data*

Our 511 tree-ring sections and cores come from seven modern forest and 49 historic building chronologies. The



DOI: 10.1002/joc

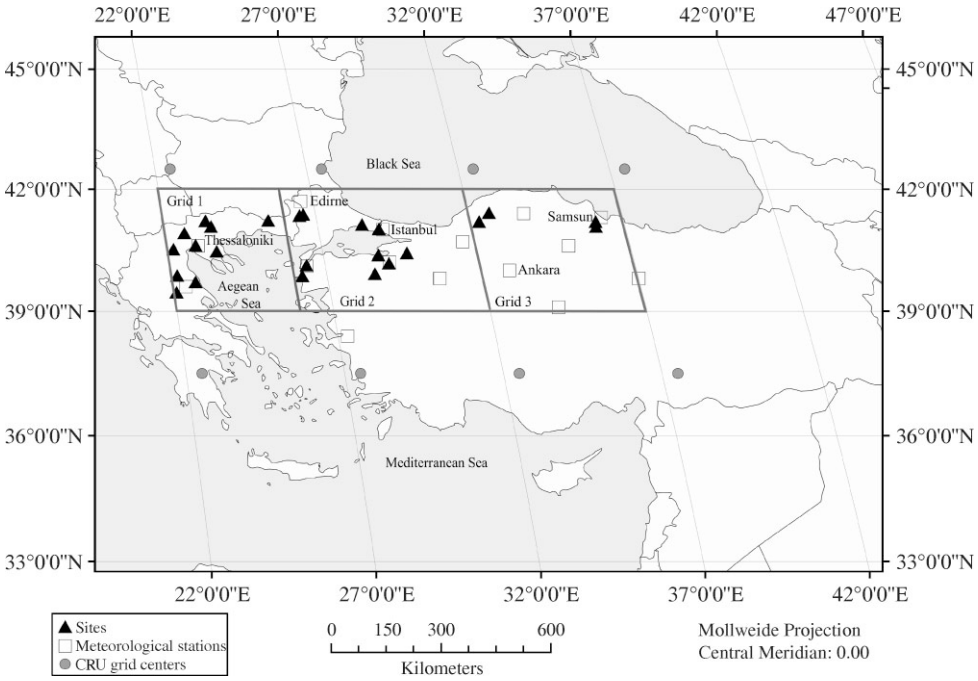


Figure 1. The locations of tree-ring sites, meteorological stations, ADP grid areas (Grids 1, 2, and 3), and the centers of 5 × 5 CRU climate grids. See Table I for site and chronology list.

historic chronologies are from 38 buildings, eight with two or more building phases or different timber sources (Figure 2; Table I) (Kuniholm and Striker, 1983, 1987; Kuniholm, 1994, 2000). The ring counts of the historic segments range from 39 to 357 rings (average 116) and the forest segments from 61 to 362 rings (average 156). Site chronologies range from 59 to 787 (average 194) years in length (Figure 2).

There is no reliable way to distinguish oak species from wood anatomy alone (Huber and von Jazewitsch, 1956, p.29; Pilcher, 1995). Seven species and subspecies were identified in six of the seven forests (Table II). They are all deciduous oaks from the subgenus *Quercus* Oersted (Schweingruber, 1990) and grow in Euxinian and sub-Euxinian mesic sites at elevations ranging from 20 to 1300 m above sea level (Zohary, 1973; Davis 1982). The southern boundaries of most of the included species' ranges are within or at the southern edge of the study region due to the general decrease in May–June precipitation from north to south (Xoplaki, 2002).

We assume that most of the historic samples' species are included in the forest species list. A secure crossdating between sites indicates that the historic sites' species contain the same common signal. The locations of the historic buildings, the secure crossdating between samples and chronologies, and the paucity or complete absence of oak samples from buildings in central and southern Turkey, outside the included oak species' ranges, imply that the timbers used in their construction were from local oaks, and that they are all mesothermic species (Davis, 1982; Zohary, 1973). If the samples are of different oak species, then those species' growth responses are very similar to the forest species' response, or the tree-ring patterns would not have crossdated securely. The inclusion of all the species in our chronology enhances the response to climate that all share in common.

Oak ring width variability is low relative to conifers and diffuse ring-porous angiosperms due to the minimum width of the necessary springwood vessels each year, approximately 0.30 mm in our samples. The vessels grow before the new leaves open in the spring (Pilcher, 1995), using the reserved material from the previous growth season to produce the needed cells. Thus, the previous year's climate parameters are possible growth-limiting factors. Pilcher found that the spring temperature of the year-before-growth correlated significantly with the rings' earlywood widths, but not highly enough to reconstruct the temperature (Pilcher and Gray, 1982). This is similar to the significant but not high correlation between our chronology and the anomalies of the precipitation of April in the year-before-growth (Figure 3). The latewood, the most variable part of annual ring growth in oaks, grows after the leaves are established, generally from May through the summer for as long as the moisture is sufficient for secondary cambial activity, and that is indicated by our chronology's response to precipitation.

Our data do not represent the full range of tree-ring widths in the oaks due to the requirement of at least 50 rings (estimated ring count at time of collection) in each sample for secure crossdating purposes. Samples with fewer than 60 rings are not included here unless they contain unique signature patterns for particular years. Therefore, samples with low ring count, generally due to larger ring widths, are absent and our ring-width measurements are in the middle-to-low range of ring widths of all oak ring growth, similar to the ring widths



DOI: 10.1002/joc

Table I. The descriptions of the 56 site chronologies from west to east: the geographical location of the site; the region, site name, and building phases (if any); beginning and ending dates, length, number of samples, and the average of correlation coefficients ($r$) between samples. An $f$ indicates a forest chronology, all others are historic building chronologies.

| Lat N | Long E | City/Region | Site Name | Site Division | Chronology Begins | Chronology Ends | Length | Sample count | Average $r$ value |
|---|---|---|---|---|---|---|---|---|---|
| ***Western grid (1): Greece*** | | | | | | | | | |
| 39.47 | 22.07 | Karditsa | Palamas, Hg. Athanasios | | 1647 | 1809 | 163 | 13 | 0.393 |
| 39.47 | 22.07 | Elasson | Panaghia Olympiotissa | | 1214 | 1335 | 122 | 7 | 0.346 |
| 40.52 | 22.18 | Verroia | Holy Apostles (Old Metropolitan) | | 1758 | 1889 | 132 | 3 | 0.414 |
| | | | Palatitsa, Hg. Demetrios | | 1628 | 1780 | 153 | 2 | 0.473 |
| | | | Tou Christou | | 1240 | 1327 | 88 | 4 | 0.468 |
| 39.72 | 22.73 | Larisa | Aghia, Hg. Panteleimon | | 1358 | 1476 | 119 | 5 | 0.422 |
| 40.62 | 22.92 | Thessaloniki | Hg. Antonios | | 1570 | 1828 | 257 | 7 | 0.346 |
| | | | Hg. Georgios (Rotonda) | Early | 1207 | 1318 | 112 | 2 | 0.470 |
| | | | | Late | 1662 | 1827 | 166 | 5 | 0.361 |
| | | | | Middle 1 | 1518 | 1588 | 71 | 2 | 0.484 |
| | | | | Middle 2 | 1350 | 1518 | 169 | 2 | 0.385 |
| | | | Hg. Aikaterini | | 1155 | 1315 | 161 | 5 | 0.400 |
| | | | Hg. Demetrios | | 1337 | 1519 | 183 | 3 | 0.502 |
| | | | Holy Apostles, Byzantine | | 1170 | 1329 | 160 | 6 | 0.433 |
| | | | Holy Apostles, Turkish porch | | 1247 | 1490 | 244 | 3 | 0.381 |
| | | | Heptapyrgion (Yedikule) | | 1373 | 1431 | 59 | 2 | 0.662 |
| | | | Hg. Sophia | | 1355 | 1521 | 167 | 7 | 0.420 |
| | | | Nikolaos Orphanos | Early | 1257 | 1458 | 202 | 1 | – |
| | | | | Late | 1614 | 1811 | 198 | 2 | 0.341 |
| | | | Nea Panaghia | | 1557 | 1832 | 276 | 26 | 0.276 |
| | | | Frourio Vardari (Octagonal Tower) | | 1478 | 1597 | 120 | 14 | 0.331 |
| | | | Metamorphosis Soter | | 1630 | 1773 | 144 | 3 | 0.359 |
| | | | Vlatadon Monastery | Early | 1199 | 1339 | 141 | 24 | 0.365 |
| | | | | Late | 1557 | 1800 | 244 | 21 | 0.309 |
| | | | White Tower | Early | 1211 | 1535 | 325 | 11 | 0.272 |
| | | | | Late | 1567 | 1847 | 281 | 14 | 0.345 |
| 41.22 | 23.37 | Thrace | Sidherokastro | | 1207 | 1327 | 121 | 4 | 0.367 |
| 41.08 | 23.52 | Serres | Prodromos Monastery | Early | 1199 | 1345 | 147 | 6 | 0.282 |
| | | | | Late | 1377 | 1497 | 121 | 6 | 0.431 |
| | | | Serres, Orestes Tower | | 1211 | 1323 | 113 | 3 | 0.413 |
| | | | Serres, Mehmet Bey Mosque | | 1322 | 1489 | 168 | 7 | 0.503 |
| | | | Serres, Zincirli Mosque | | 1406 | 1492 | 87 | 3 | 0.523 |
| 40.47 | 23.57 | Chalkidiki | Arnaia, Barbara, Koutri Chorafi | $f$ | 1740 | 1979 | 240 | 10 | 0.296 |
| 41.23 | 25.42 | Livadia | Paterma Forest, Komotini | $f$ | 1840 | 1979 | 140 | 12 | 0.355 |
| ***Center grid (2): Greece*** | | | | | | | | | |
| 41.35 | 26.47 | Didymoteichon | Didymoteichon, Vayazit Mosque | | 1186 | 1495 | 310 | 30 | 0.305 |
| 41.38 | 26.60 | Pythion | Pythion Castle | | 1209 | 1331 | 123 | 5 | 0.243 |
| ***Turkey*** | | | | | | | | | |
| 39.87 | 26.20 | Çanakkale | Üvecik, Cezayirli Hasan Paşa Köşkü | | 1627 | 1782 | 156 | 5 | 0.416 |
| 40.13 | 26.40 | | Kilid ul-Bahir Castle | | 1295 | 1462 | 168 | 21 | 0.311 |
| 41.13 | 28.45 | İstanbul | Belgrade Ormanı | $f$ | 1769 | 1985 | 217 | 26 | 0.319 |
| 39.92 | 28.55 | Bursa | Mustafakemalpaşa, Devecikonağı | $f$ | 1773 | 1985 | 213 | 19 | 0.238 |
| 40.38 | 28.78 | | Mudanya, Tirilye, Kemerli Kilise | | 1198 | 1336 | 139 | 8 | 0.306 |
| 41.02 | 28.97 | İstanbul | Kariye Camii | Late | 1189 | 1308 | 120 | 12 | 0.373 |
| | | | Beyoğlu, Karaköy Vapur İskelesi | Black Sea | 1602 | 1852 | 251 | 4 | 0.234 |
| | | | | Thrace | 1721 | 1857 | 137 | 8 | 0.354 |
| | | | Ayasofya, Bannister | | 1394 | 1581 | 188 | 8 | 0.342 |
| | | | Ayasofya, NW Buttress | | 1188 | 1332 | 145 | 8 | 0.350 |
| | | | Ayasofya, Türbe | | 1356 | 1615 | 260 | 7 | 0.334 |
| 40.18 | 29.07 | Bursa | I. Murat Hüdavendiğâr Camii | | 1111 | 1384 | 274 | 7 | 0.359 |
| 40.43 | 29.72 | Bilecik | İznik, Elbeyli, Mara Camii | | 1398 | 1554 | 157 | 6 | 0.194 |
| | | | İznik, Nilüfer İmareti | | 1136 | 1375 | 240 | 6 | 0.353 |
| | | | İznik, Hg. Sophia | | 1081 | 1241 | 161 | 4 | 0.349 |
| 40.23 | 30.00 | | Vezirhan | | 1526 | 1657 | 132 | 4 | 0.382 |




DOI: 10.1002/joc

Table I. (*Continued*).

| Lat N | Long E | City/Region | Site Name | Site Division | Chronology Begins | Chronology Ends | Length | Sample count | Average *r* value |
|---|---|---|---|---|---|---|---|---|---|
| ***East grid (3): Turkey*** | | | | | | | | | |
| 41.20 | 32.28 | Zonguldak | Yenice, Bakraz Bölgesi | *f* | 1623 | 1984 | 362 | 10 | 0.327 |
| 41.42 | 32.67 | | Karabük, Büyükdüz Ormanı | *f* | 1699 | 1985 | 287 | 10 | 0.390 |
| 41.08 | 36.05 | Samsun | Kavak, Çakallı Mevkii | *f* | 1835 | 1989 | 155 | 17 | 0.386 |
| 41.08 | 36.15 | Samsun | Kavak, Bekdemirköy, Cami | | 1089 | 1875 | 787 | 41 | 0.373 |
| | | | | | Total | | 10 576 | 511 | |
| | | | | | Average | | 189 | 9 | 0.370 |

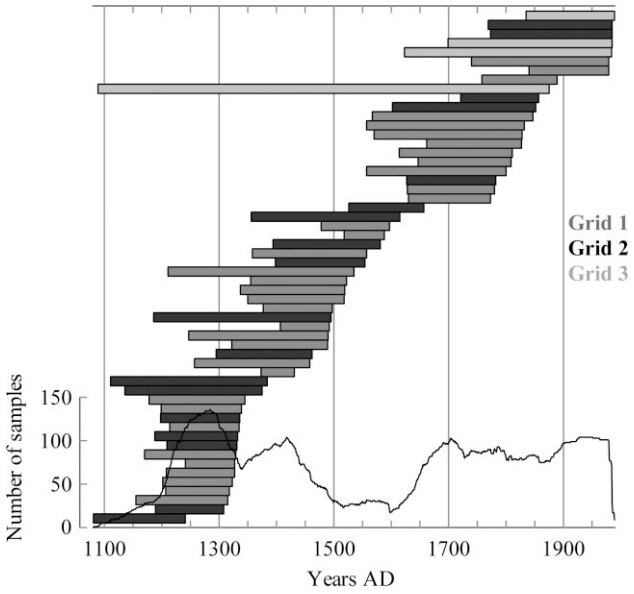


Figure 2. The temporal location of the historic and forest chronologies and the number of samples included over time. The grid represented by each forest and historic building is indicated by the shade of gray. See Figure 1 for site locations.

Table II. The *Quercus* species of the forest samples.

| |
|---|
| *Q. frainetto* Ten. (= *Q. conferta* Kit.) |
| *Q. hartwissiana* Steven. |
| *Q. petraea* (Mattuschka) Lieb. |
| *Q. petraea iberica* (Steven ex Bieb.) Krassilin (= *Q. dschoruchensis* C. Koch) |
| *Q. petraea petraea* (= *Q. sessiliflora* Salisb.) |
| *Q. robur* L. |

in the historic samples of Norway spruce noted in Wilson *et al*. (2004).

The historic wood has no provenance other than the buildings' locations: in our regional context, this is not important (Kelly *et al*., 1989). The buildings' locations and the more secure crossdating between site chronologies within each of the three grids imply that there was little or no transportation of oak timbers from very far outside the study region. In larger cities, such as Thessaloniki and Istanbul, transport may have been necessary at the times of extensive building, especially in the early fourteenth, late fifteenth to early sixteenth, and late eighteenth to early nineteenth centuries, but the correlations between the included chronologies of each city area do not indicate long-distance transport to any great extent. Oak forests are still located around the region today, albeit in smaller numbers. The dendrochronology of historic buildings such as Haghia Paraskevi, a Gothic (*i.e*. Frankish) church in Chalkis, Greece (Kuniholm, 2004; Hammond, 2005), that was constructed of Alpine larch is one exception that 'proves' the rule. Any chronology from such a building is not included in the regional chronology since it does not crossdate with the other local site chronologies.

At each forest site, at least 10 sections were collected from forest timbers or stumps. At the historical sites, sections and cores were collected in whatever quantity was available. Seven historical sites have more than one site chronology from different building phases and one site has two chronologies from either two oak species or two timber sources.

Each sample's ring widths are measured twice: the measurements are reconciled to at least 97% accuracy with the same positive or negative signs in the differences between year-to-year ring widths. Two or more radii are measured from samples with visible differences in ring widths around their circumference, otherwise one radius is measured.

For crossdating purposes, the measurements of each site's samples are detrended with mainly negative exponential curves in order to preserve long-term variance that samples have in common as well as their year-to-year variance. In general, detrending removes an individual tree's unique response and equalizes the variance in ring widths over its lifespan (Cook and Kairiukstis, 1990; Cook and Peters, 1997). The detrended sample measurements from each historic site are crossdated with each other using the Student's *t*-test, trend coefficients, and visual fits to establish their relative dates. The calendar date of the outer ring of each forest tree is known from the year and season in which it was felled, and all its rings are calendar-dated according to that year. The dated samples from each site or forest that securely crossdate with each other (within site) are averaged into a site chronology, with the trees equally weighed. Each historic site chronology is then crossdated with the forest and other dated



DOI: 10.1002/joc

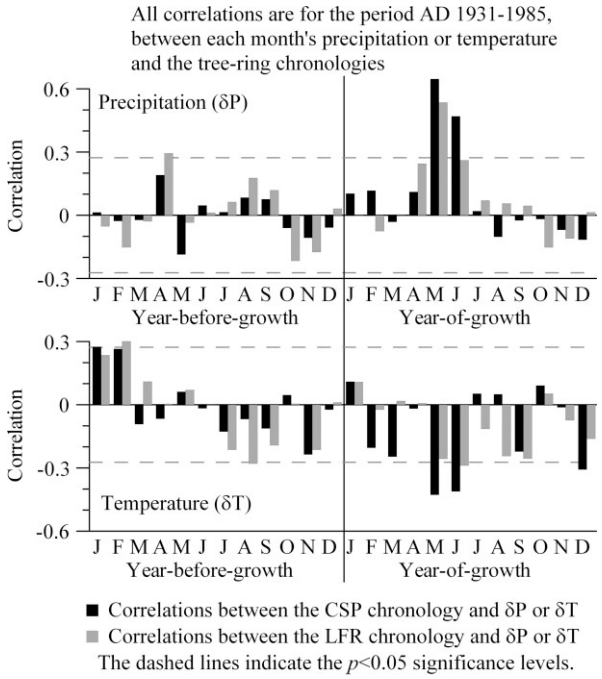


Figure 3. Shown here are the correlation coefficients between the time series of precipitation or temperature anomalies for each month of the year-before-growth and the year-of-growth and the two tree-ring chronologies. The ADP grids' climate data is used here, and the two tree-ring chronologies are composed of the same samples with different detrending methods: the cubic spline normalized site chronology (CSP) and the low-frequency-retained chronology (LFR). The bars indicate the high positive correlations with May and June precipitation, negative correlations with the May and June temperature, and the reduced but significant effects of the precipitation of April in the year-before-growth and the temperatures in the winter and summer months in the year-before-growth. Also of importance here are the higher correlations of the cubic spline chronology with the May and June parameters. For the months with reduced but significant correlations, the correlation is generally higher with the low-frequency-retained chronology.

chronologies to determine its correct calendar dates (Baillie and Pilcher, 1973; Fritts, 1976; Pohl, 1995). The averages of the Pearson correlation coefficients ($r$) between the samples within each of the 56 site chronologies are listed in Table I. Figure 2 shows the 56 site chronologies, their distribution, and the total sample number over time. The average correlation coefficients between samples and between site chronologies are listed in Table III.

For a regional climate reconstruction, the oak ring widths were detrended by fitting a cubic spline curve to each sample's raw measurements, which reduces low-frequency variance and enhances annual variance. The questions of what parameters to use in specifying the fit of the spline curve (minimum least-squares fit, or frequency response and wavelength of minimum rigidity), and whether the chosen parameter(s) should be the same for all the samples or determined by each sample's length and variance were addressed (Cook and Kairiukstis, 1990, p. 112). Smoothed cubic-spline curves were fitted by the software program CORINA (software available at http://dendro.cornell.edu/) using a minimum sum of residual variance of $e^{-16}$ as the limit to the amount of variance explained by a curve fitted to each sample (Cook and Peters, 1997). ARSTAN (Cook and Holmes, 1999) was used to fit a spline curve with the minimum rigidity of 28 years, 50% frequency response to each sample's measurements.

Each sample's measurements were detrended by dividing them by the corresponding values in the fitted Cubic Spline curve (CSP), a process which equalizes the average ring width of the samples. For one method chronology, the ARSTAN CSP sample chronology, each sample was detrended in the ARSTAN program, as described in the preceding text, and the detrended data were averaged. For the CORINA method chronologies, each sample was detrended by CORINA, as described in the preceding text. For the CORINA CSP sample chronology, the CORINA-detrended sample data were averaged. The CORINA-detrended sample data were also used in two other methodology tests to determine whether normalizing the data would enhance the recorded common signal. For the CORINA CSP normalized sample chronology, each sample's detrended data were normalized, and the normalized data was averaged; and, for the CORINA CSP normalized site chronology, the detrended data of the samples from each site were averaged into site chronologies, then the site chronologies were normalized and averaged. For an evaluation of what low-frequency common variance is removed by detrending with the spline curves, the conservatively detrended sample data used for crossdating purposes were also averaged into site chronologies, and the site chronologies were averaged into the low-frequency-retained (LFR) tree-ring chronology.

The temporal variance over each chronology was adjusted according to the number of samples or site chronologies and the average of correlation coefficients between the samples or site chronologies contained in each year (Osborn *et al.*, 1997, p.94, equation 7). This adjustment reduced the amplitude of variance in the

Table III. Averages of the correlation coefficients ($r$) and number of correlations ($N$) between the tree-ring samples and between site chronologies from the three grids.

| Samples within | | | Samples outside of | | All samples | | Site chronologies within | | | Site chronologies from | | |
|---|---|---|---|---|---|---|---|---|---|---|---|---|
| | $r$ | $N$ | $r$ | $N$ | $r$ | $N$ | | $r$ | $N$ | | $r$ | $N$ |
| Grid 1 | 0.399 | 1645 | 0.188 | 6473 | 0.231 | 8118 | Grid 1 | 0.300 | 169 | Grids 1 and 2 | 0.214 | 118 |
| Grid 2 | 0.321 | 1341 | 0.149 | 4346 | 0.190 | 5687 | Grid 2 | 0.293 | 60 | Grids 2 and 3 | 0.259 | 30 |
| Grid 3 | 0.379 | 644 | 0.213 | 689 | 0.293 | 1333 | Grid 3 | 0.409 | 5 | Grids 1 and 3 | 0.141 | 60 |



DOI: 10.1002/joc

periods of low sample count in the early years of the chronologies and to a lesser extent in the fifteenth through early seventeenth centuries. It also added a small amount of amplitude to the chronology in all of the twentieth century, a result of the increase in average biological age of the rings with the addition of very few samples in that period. From the very small differences between values in the original and adjusted chronologies, it is evident that the number of samples is large enough for accurate values for most of its length. The only period for which it is significantly adjusted is when the sample number is less than 25 and when the chronology is composed mostly of juvenile growth rings, and that occurs only in the first century of the chronology, A.D. 1081–1168.

*Climate data*

Monthly precipitation and temperature anomalies ($\delta P$ and $\delta T$, respectively) for the grids indicated in Figure 1 were calculated from meteorological station data available at the National Climatic Data Center/National Oceanographic and Atmospheric Administration's website, http://www.ncdc.noaa.gov/oa/ncdc.html, on the Global Historical Climatology Network page. The 15 stations used here (Table IV) all contain monthly values for 1931–1985, 13 with long precipitation records and 8 with long temperature records. Two stations contain a few missing values that were replaced with the averaged value from the two or three closest stations.

Gridded monthly precipitation and temperature data in eight 5 latitude by 5 longitude grids for the region 35 –45 N latitude and 20 –40 E longitude were also downloaded from the Climate Research Unit (CRU) website http://www.cru.uea.ac.uk/(Hulme, 1992, 1994; Hulme *et al*., 1998) for a comparison with the tree-ring and station data. The CRU precipitation grids begin in 1900, an advantage over the station data discussed earlier. However, caution was used with the data from 1900 to 1930 since the available data were limited to two stations north of 42 N and west of the Black Sea, plus a few stations from outside the region with interpolation. Temperature data available from the same eight grids begin at dates ranging from the late 1800s up to 1927 and all end in 1998.

The monthly precipitation values of all the station and gridded data sets were transformed to square root values

Table IV. A. The correlation coefficients and sign tests between the five method chronologies and May–June precipitation anomalies for 1931–1985 and 1900–1989, calculated from the Climate Research Unit's data for four grids, 40–45 N, 20–40 E. The 1931–1985 period contains the most complete meteorological data set for the region, and is restricted at 1985 by the low number of samples in the tree-ring data after that. The 1900–1989 set, the complete length shared by the CRU data and the tree-ring chronology, is used for comparison. Any correlation below 0.632 explains less than 40% of the variance. The normalized chronology has a slightly higher correlation with the May–June $\delta P$, but not significantly higher. The sign test is determined by the how many of the signs (positive or negative) of the subtraction of consecutive years' values are the same between the tree-ring chronology and the May–June precipitation anomalies. The detrending methods used in the CORINA and ARSTAN programs are discussed in the text. B. The correlation coefficients for the three periods of regression analysis, calibration, and verification (represented by the Roman numerals) between the five chronologies and the averages of the May–June precipitation anomalies from the four CRU grids at 40–45 N, 20–40 E and the three ADP grids of 39–42 N, 22–37 E. The two periods of post-1930 data were chosen to split the data into segments that have a relatively equal response to May–June precipitation. The 1900–1930 sequence was used to verify that the analysis is valid, which it does despite the limited meteorological data available prior to 1931. All values are at the $p < 0.05$ probability level.

| **A.** Detrending Method | Correlation 1931–1985 | Correlation 1900–1989 | % sign agreement 1931–1985 | % sign agreement 1900–1989 |
|---|---|---|---|---|
| With Cubic SPline curve: | | | | |
| Corina CSP sample | 0.775 | 0.618 | 0.852 | 0.730 |
| Corina CSP norm sample | 0.773 | 0.611 | 0.815 | 0.730 |
| Corina CSP norm site | 0.781 | 0.636 | 0.759 | 0.663 |
| ARSTAN CSP sample | 0.764 | 0.600 | 0.796 | 0.708 |
| Low frequency retained | 0.543 | 0.495 | 0.759 | 0.663 |

| **B.** Detrending Method | 1941–1970 (I) | | 1931–1940, 1971–1985 (II) | | 1900–1930 (III) |
|---|---|---|---|---|---|
| | CRU MJ $\delta$P | ADP MJ $\delta$P | CRU MJ $\delta$P | ADP MJ $\delta$P | CRU MJ $\delta$P |
| With cubic spline curve: | | | | | |
| Corina CSP sample | 0.762 | 0.591 | 0.821 | 0.724 | 0.528 |
| Corina CSP norm sample | 0.762 | 0.594 | 0.819 | 0.724 | 0.492 |
| Corina CSP norm site | 0.788 | 0.613 | 0.786 | 0.673 | 0.547 |
| ARSTAN CSP sample | 0.735 | 0.558 | 0.818 | 0.715 | 0.451 |
| Low frequency retained | 0.749 | 0.550 | 0.515 | 0.414 | 0.509 |



DOI: 10.1002/joc

in order to correct a slight skewdness. The skewdness is due to the distribution of the amount of precipitation in a semiarid environment over time: their median values are consistently less than their mean values. This feature is most evident temporally in the rainfall of the late spring and summer months, and spatially in the western grids. The distribution of the square-rooted values is more similar to that of the tree-ring widths than the distribution of the actual precipitation. Anomalies were then calculated from the monthly averages and standard deviations of the square-rooted precipitation values for the period in common, 1931–1985. The monthly temperature data were each converted to anomalies in degrees centigrade by subtracting the average of their monthly values for 1931–1985.

The stations' monthly values were weighted using Thiessen polygons (Jones, 1988) over the original 3 latitude by 5 longitude grids in the region (Figure 1), with one outer station's temperature data used for latitudinal depth, and then averaged together for the region's anomalies. These gridded precipitation and temperature data sets are hereafter referred to as the 'ADP' (Aegean Dendrochronology Project) grid data.

Both the CRU precipitation and temperature data sets were converted to anomalies in the same way as the ADP grids noted in the preceding text. The anomalies of the eight CRU grids were averaged, along with the anomalies in the four CRU grids in each latitude segment, 35–40 N and 40–45 N.

A comparison between the ADP and the CRU precipitation anomalies indicated that the CRU 40–45 N 20–40 E data sufficiently represent the precipitation anomalies of the study region ($r = 0.823$) despite the additional 3 degrees of latitude to the north that is included in the CRU grid. The correlation between the ADP $\delta P$ and the CRU 35 –40 N latitude $\delta P$ data is lower, at 0.706, and the correlation between the ADP $\delta P$ with average of the eight CRU grids' $\delta P$ is between the two. The longer period of the CRU data, plus the equally high correlation with the oak chronology, justified the use of the CRU $\delta P$ 40–45 N latitude data for this study, despite the caveat noted above. The CRU $\delta T$ data, however, do not significantly correlate with either the ADP $\delta T$ data or the tree-ring chronologies; the station and ADP grids' temperature anomalies are used in the following text.

### *A comparison of the precipitation record in the five method chronologies*

Tests between the five methods' chronologies included each chronology's correlation coefficient and sign test with the May–June $\delta P$ (Table V). Between the four cubic spline chronologies and the May–June $\delta P$, there are no significant differences in the results of the methodology over the calibration period or in shorter periods. The number of samples outweighs the importance of the methodology in this study, but the chronology constructed of the normalized site data correlates slightly higher and consistently over time with the May–June $\delta P$, which may indicate that both the normalization and the use of the site chronologies (rather than sample data) enhances the

Table V. Meteorological stations, their locations, and the percent of the grids' area that is unique to each. The percent is equal to 100 times the weight used in calculating the respective grids' anomalies. The three grids' anomalies were averaged into the regional ADP precipitation and temperature anomaly data sets. The Izmir station is not in the study region but was added for latitudinal depth.

| Stations | Lat N | Long E | Alt m | Percent of each grid represented by the station | | | | | |
|---|---|---|---|---|---|---|---|---|---|
| | | | | Precipitation | | | Temperature | | |
| | | | | G1 | G2 | G3 | G1 | G2 | G3 |
| *Greece* | | | | | | | | | |
| Larisa | 39.6 | 22.4 | 73 | | | | 11.2 | | |
| Thessaloniki | 40.6 | 23 | 30P, 4T | 52.5 | | | 45.9 | | |
| *Turkey* | | | | | | | | | |
| Çanakkale | 40.1 | 26.4 | 3 | 30.4 | 9.6 | | | | |
| Edirne | 41.7 | 26.6 | 48 | 17.1 | 6.2 | | 33.3 | 9.2 | |
| Izmir* | 38.4 | 27.3 | 25 | | | | 9.6 | 11.2 | |
| Istanbul | 41 | 29.1 | 40 | | 23.7 | | | 59.6 | |
| Bursa | 40.2 | 29.1 | 100 | | 22.1 | | | | |
| Eskişehir | 39.8 | 30.6 | 783 | | 17.1 | | | | |
| Bolu | 40.7 | 31.6 | 742 | | 20.0 | 5.8 | | | |
| Ankara | 40 | 32.9 | 894 | | 1.3 | 18.4 | | 20.0 | 53.8 |
| Kastamonu | 41.4 | 33.8 | 799 | | | 18.3 | | | |
| Kirşehir | 39.1 | 34.2 | 985 | | | 10.8 | | | |
| Çorum | 40.6 | 35 | 837 | | | 20.4 | | | |
| Samsun | 41.3 | 36.3 | 44 | | | 15.0 | | | 29.1 |
| Sivas | 39.8 | 37 | 1285 | | | 11.3 | | | 17.1 |



DOI: 10.1002/joc

regional climate signal contained in the master chronology.

The process of using the minimum residual-fit curve for detrending each sample rather than a curve of the same wavelength and rigidity for detrending all samples (CORINA *vs* ARSTAN; either can be done with ARSTAN) appears to produce optimal results (Table V), but again it is an insignificant increase. Extensive testing with limited data sets is necessary to assess the methodological nuances.

From these tests, we decided to use the cubic spline chronology composed of the normalized site chronologies for the May–June $\delta P$ reconstruction and to compare it with the low-frequency-retained chronology to determine what was removed by these detrending methods. The normalized site chronology was chosen not only because of the high values discussed in the preceding text but also for the equal weighting of the different site chronologies over time. The LFR chronology has lower values of the correlation coefficient and the sign test with the May–June $\delta P$, but both values are statistically significant (Table V). The differences between the two chronologies and their record of the May–June $\delta P$ are discussed in the following text.

*Calibration, verification, and reconstruction*

Correlations between the chosen CSP method chronology, the LFR chronology, and the monthly CRU precipitation and ADP temperature anomalies of the year-before-growth and the year-of-growth were calculated for 1931–1985 (Figure 3). May and June precipitation is clearly the major growth-limiting factor with the precipitation of April in the year-before-growth plus the mean temperatures of May and June as other possible growth-limiting forces.

A regression analysis with the tree-ring chronology as the predictand and the May and June $\delta P$ as the predictors both give approximately the same weight, thus both have about the same effect on the tree-ring growth in that period. Combining the two variables to use as a single predictor slightly increased the variance explained. Additions of the other significantly correlated parameters add small amounts to the variance explained, but not consistently over time.

For 1931–1985, the CSP chronology was divided into two sequences for verification and calibration of the reconstructed values (Figure 4). One sequence consisted of 1941–1970 and a second segment included a split sequence of 1931–1940 and 1971–1985. The two groups have an approximately equal response to the May–June precipitation. A third sequence containing the years 1900–1930 was used for verification alone. For each sequence, the chronology was used as the predictor to calculate the coefficients of a regression equation with the May–June precipitation anomalies as the predictand. The two regression equations were tested with the other sequence for verification. The coefficients for the final reconstruction equation were calculated from the values of 1931–1970 due to the reduced amount of available climate data prior to 1931 plus the reduced regional response in 1971–1980 (Figure 4), which appears to be the result of more variance in the precipitation from east to west than in other years. The two years of 1936 and

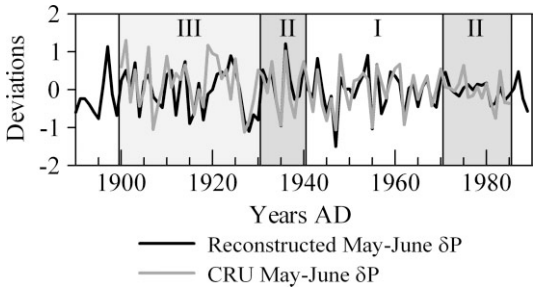


Figure 4. The May–June precipitation anomalies and the normalized site chronology (correlation coefficient = 0.636). The periods used for calibration and verification include the following: I. 1941–1970; II. 1931–1940 and 1971–1985; and III. 1900–1930 (see text and Table VB for correlation values within the periods).

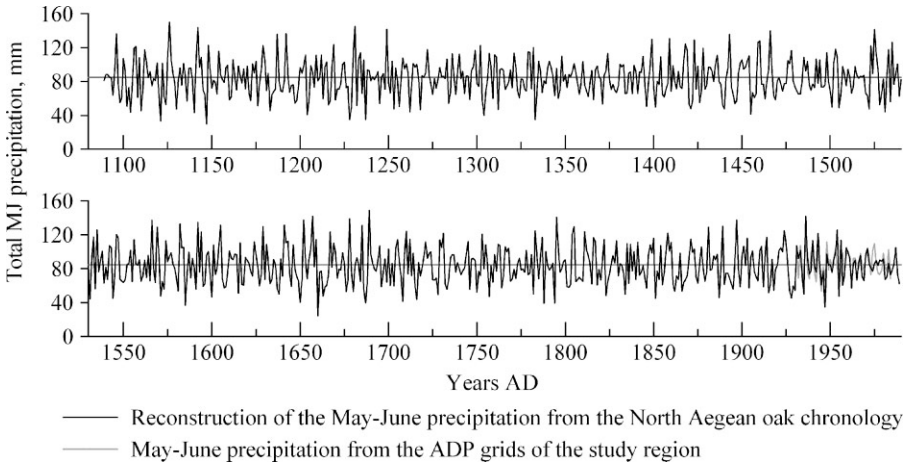


Figure 5. The A.D. 1089–1989 May–June precipitation reconstructed from the North Aegean oak tree-ring chronology and the May–June precipitation averaged from the ADP grids of the study region. The average of the May–June precipitation from the CRU grids is about 25 mm higher than the average for the stations in the study region; thus, the average May–June precipitation of stations within the study region was used for calculating the reconstruction.



DOI: 10.1002/joc

1947, whose values statistically had the most influence, were also removed for a better reconstruction of the majority of the data set. Correlation coefficients and sign tests were used to corroborate the fit with the May–June $\delta P$ and the first-year differences (positive or negative) between the data sets (Table V, Figure 4) (Cook and Kairiukstis, 1990; Gordon, 1982). The May–June precipitation anomalies were then reconstructed from the complete chronology and converted into precipitation values for the region from 1089 to 1989.

## RESULTS AND DISCUSSION

### *The May–June regional precipitation reconstruction*

The values of the reconstructed regional May–June precipitation, A.D. 1089–1989, are shown in Figure 5 and are available on the NOAA website http://www/ncdc.noaa.gov/paleo/recons.html. They correlate significantly ($p < 0.05$) with the May–June precipitation anomalies of 11 of the 13 stations within the study area (Table VI). The highest correlations are with the station data of Thessaloniki (Grid 1), Edirne (Grid 2), and Samsun (Grid 3), indicating that the reconstruction represents the regional precipitation. The two insignificant correlations are with the May–June precipitation of the two stations at the minimum and maximum elevations of the oak species' ranges: 3 m elevation on the east Aegean Sea coast (Çanakkale), and 1285 m elevation on the eastern boundary of the study region (Sivas) on the Anatolian Plateau.

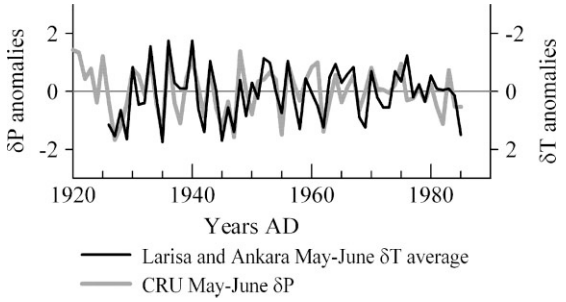


Figure 6. The averaged Larisa (Greece) and Ankara (Turkey) May–June temperature and the CRU May–June precipitation anomalies have a correlation coefficient of −0.680, an indication of the close relationship between the May–June precipitation and temperature in the interior of this region. The scale on the temperature anomalies axis to the right is reversed.

Table VI. Correlations between our reconstructed May–June precipitation and the meteorological stations' May–June $\delta P$ for 1931–1985.

| Stations | Alt (m) | *r*-scores with CRU 20–40 E May–June $\delta P$ | *r*-scores with reconstructed May–June $\delta P$ |
|---|---|---|---|
| Thessaloniki | 30 | 0.545 | 0.513 |
| Çanakkale | 3 | 0.559 | 0.257[b] |
| Edirne | 48 | 0.676 | 0.547 |
| Istanbul | 40 | 0.565 | 0.313[a] |
| Bursa | 100 | 0.639 | 0.434 |
| Eskişehir | 783 | 0.543 | 0.378 |
| Bolu | 742 | 0.583 | 0.384 |
| Ankara | 894 | 0.451 | 0.306[a] |
| Kastamonu | 799 | 0.621 | 0.499 |
| Kirşehir | 985 | 0.369 | 0.270[a] |
| Çorum | 837 | 0.452 | 0.349 |
| Samsun | 44 | 0.587 | 0.567 |
| Sivas | 1285 | 0.241[a] | 0.219[b] |

Note: All probability is at the level of $p < 0.01$ unless superscripted [a] ($p < 0.05$) or [b] ($p > 0.05$).

### *Growth response to May–June temperature*

Any growth response of the oaks to May–June temperature is due to the close inverse relationship between precipitation and temperature in this warm subhumid climate regime. An increase in precipitation means more clouds, less direct heat, lower temperature, and less evaporation (Griffiths and Driscoll, 1982), with more water available to the trees (Kramer and Kozlowski, 1979) and *vice versa*. The variance explained in the chronologies by the regional May–June average temperature anomalies is less than 30%. However, the May–June temperature anomalies of two interior stations in the outer grids, Larisa (Greece) and Ankara (Turkey), correlate significantly with the regional May–June $\delta P$ at −0.508 and −0.634, respectively. In a regression equation, the two explain 44.8% of the variance in the tree-ring chronology. The response of the oaks to temperature is not sufficient to reconstruct the regional May–June $\delta T$ accurately, but the reconstruction of the May–June precipitation anomalies may be regarded as an inverse of the approximate values of the May–June temperature anomalies in Ankara and Larisa over time (Figure 6).

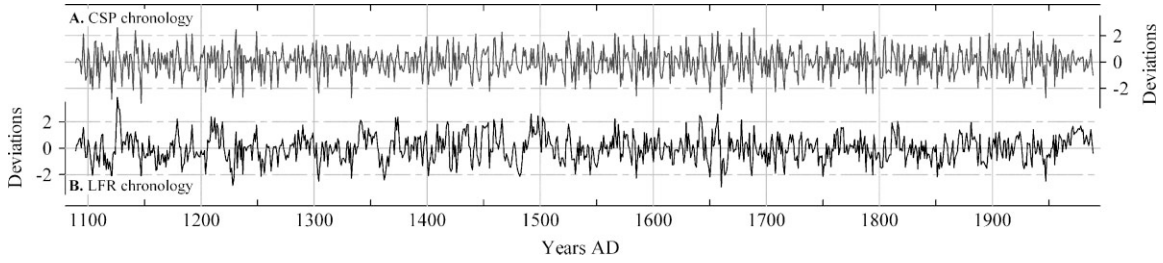


Figure 7. A comparison of the Cubic SPline chronology (used in the reconstruction) and the low-frequency-retained chronology. It is clear from a visual inspection of the two chronologies that the low-frequency signal is lacking in our reconstruction. However, its higher correlation with the regional precipitation indicates that the cubic spline chronology contains a valid record of the regional variability of the May–June precipitation.



DOI: 10.1002/joc

*The precipitation record and history*

The significance of the years of high and low values in the reconstructed May–June precipitation were examined by comparing the cubic spline chronology with the low-frequency-retained chronology to assess their similarities and differences due to the detrending processes (Figure 7). The difference between the two chronologies is mainly in their amplitudes during certain years. The removal of the low-frequency signal may either enhance or ameliorate the severity of each extreme, depending on the surrounding values. Amelioration can be seen in the years 1479–1485, a period of severe drought, and enhancement in 1545–1547 (Figure 7). Sustained periods of extremely low or high May–June precipitation (more than 2 standard deviations above or below the mean) for two or more years occur only in the LFR chronology (Table VII). However, there are many extended periods of more modest positive and negative extremes (values above or below 1 standard deviation from the mean) and they are also more apparent in the LFR chronology. The frequency of extremes is greatest in the middle of the chronology, from the fifteenth through the seventeenth centuries, which may be an indicator of the influence of the Little Ice Age in this region (Grove, 2004; Grove and Grove, 1992; Fagan, 2000). A comparison between the years of the extremes in the reconstruction and the historical climate record was attempted, but the latter is very limited in this area (Grove, 2004; Fagan, 2000; Lamb, 1995). The historical record of famine in our region noted in Kuniholm (1990) for 1873–1874 and for many of the years between 1564–1612 is occasionally also recorded as a drought in the tree rings (e.g. 1584–1585), but at least one half of these years does not show any small ring growth (e.g. 1574–1576). The historically reported 'years of famine' may indicate a lack of precipitation in the total months of the growing season rather than May and June alone and only affect a local area, or they could possibly be a reaction to the relatively poor growth following a number of years of high precipitation. Years of extreme tree-ring growth in the Black Sea–Ankara region noted in Akkemik *et al*. (2005) since 1635 are represented 70% of the time in the regional chronology, though not always at the same magnitude (see Table VII), and 76.9% of the signature years since 1881 listed in Hughes *et al*. (2001) are likewise represented.

The increase in relative ring widths since 1950, removed by the cubic spline detrending but evident in the LFR chronology (Figure 7), does not reflect an increase in the May–June precipitation anomalies (Figure 4). The influence of other parameters, including possible human impact, is under examination to see if the cause can be determined. Similarly, periods with extreme spatial variation in tree-ring growth resulting in flat segments of the tree-ring chronology such as in the 1770s and 1970s are under scrutiny for the possible cause. The flatness of the chronology in the 1970s reflects an increase in the spatial variation of the May–June precipitation, with only the data from the grids of north-central Turkey (30–35 E and 35–40 E) having a significant correlation, but the question of why this occurs needs further analysis. Answers to these questions are essential for an accurate interpretation of the long-term climate record contained in a tree-ring chronology along with historical and other proxy data sets.

Table VII. The years where values of the CSP and LFR chronologies were either above or below the mean by two standard deviations. There is more difference between the two in the wet than in the dry years: only four of the 33 years are in common with the wet years, 12 out of 27 drought years. The CSP also reduced the number of consecutive years in the extreme data sets from 5 to none.

| Extreme drought years | | Extremely wet years | |
|---|---|---|---|
| LFR | CSP | LFR | CSP |
| 1104 | | 1126 | 1126 |
| 1121 | 1121 | 1127 | |
| | | 1128 | |
| 1147 | 1147 | | 1142 |
| | | 1179 | |
| | 1204 | 1209 | |
| 1228 | 1228 | 1212 | |
| 1229 | | 1219 | |
| | 1237 | | 1231 |
| 1253 | | | 1249 |
| 1304 | 1304 | 1341 | |
| 1333 | 1333 | 1342 | |
| 1362 | | 1372 | |
| | | 1374 | |
| 1401 | | 1418 | |
| | | | 1443 |
| | 1455 | 1459 | |
| | | 1466 | 1466 |
| 1482 | | 1492 | |
| | | 1498 | |
| | | 1502 | |
| | | 1503 | |
| 1544 | | | 1525 |
| 1585 | 1585 | 1566 | |
| | | 1641* | |
| | | 1642 | |
| 1650 | 1650 | | 1652 |
| 1660* | 1660* | 1657 | 1657 |
| 1663 | | 1678* | 1678* |
| 1687* | 1687* | | 1689 |
| | 1708* | | |
| 1716 | 1716 | | |
| 1750 | | | |
| | 1788 | | |
| 1794 | 1794 | | 1795 |
| 1851 | | 1816* | |
| 1947 | 1947 | | 1936 |

* The extreme years since 1635 that are listed in Akkemik *et al*. (2005) and that are also extreme here. Seventy percent of the years in that list are of the same sign in our reconstruction, but not of the same amplitude due to the differences in local *versus* regional reconstructions.




DOI: 10.1002/joc

Table VIII. Correlation coefficients ($r$) and probability levels ($p$) between reconstructed precipitation data sets and precipitation anomalies of various grids and monthly combinations from in and around our study region. A. Correlations between the reconstructions for the length shared by the two sets. B. Correlations between the indicated sets for 1900–1989. Bold numbers are the values for the correlation with the particular CRU grid, or combined set of grids, that is the closest to the origin of the included tree-ring chronologies.

**A.** Correlation for periods in common

| | | Our | A05 | D01 | T03–1339 |
|---|---|---|---|---|---|
| *Precipitation reconstructions* | | May–Jun | Mar–Jun | Feb–Jun | May–Jun |
| Akkemik *et al*. (2005) | $r$ | 0.429 | | | |
| March–June, 1635–2001 [A05] | $p$ | 0.000 | | | |
| D'Arrigo and Cullen (2001) | $r$ | 0.390 | 0.465 | | |
| February–June, 1628–1980 [D01] | $p$ | 0.000 | 0.000 | | |
| Touchan *et al*. (2003) | $r$ | 0.193 | 0.240 | 0.716 | |
| May–June, 1339–1998 [T03–1339] | $p$ | 0.000 | 0.000 | 0.000 | |
| Touchan *et al*. (2003) | $r$ | 0.245 | 0.177 | 0.754 | 0.922 |
| May–June, 1776–1998 [T03–1776] | $p$ | 0.000 | 0.008 | 0.000 | 0.000 |

**B.** Correlations for 1900–1989

| | | Reconstructions from tree-ring chronologies | | | | |
|---|---|---|---|---|---|---|
| | | Our | A05 | D01 | T03–1339 | T03–1776 |
| | | May–Jun | Mar–Jun | Feb–Jun | May–Jun | May–Jun |
| *Gridded δP instrumental data* | | | | | | |
| May–June δP 20–40 E, 40–45 N | $r$ | **0.631** | 0.489 | 0.458 | 0.392 | 0.409 |
| (used for our reconstruction) | $p$ | **0.000** | 0.000 | 0.000 | 0.000 | 0.000 |
| March–June δP 30–35 E, 40–45 N | $r$ | 0.483 | **0.561** | 0.329 | 0.198 | 0.203 |
| | $p$ | 0.000 | **0.000** | 0.003 | 0.061 | 0.055 |
| March–June δP 20–40 E, 40–45 N | $r$ | 0.491 | **0.519** | 0.317 | 0.180 | 0.189 |
| | $p$ | 0.000 | **0.000** | 0.004 | 0.090 | 0.075 |
| February–June δP 20–40 E, 40–45 N | $r$ | 0.466 | 0.500 | 0.254 | 0.134 | 0.145 |
| | $p$ | 0.000 | 0.000 | 0.022 | 0.209 | 0.173 |
| May–June δP 25–30 E, 35–40 N | $r$ | 0.415 | 0.390 | 0.587 | **0.574** | **0.577** |
| | $p$ | 0.000 | 0.000 | 0.000 | **0.000** | **0.000** |
| May–June δ P 20–40 E, 35–45 N | $r$ | 0.556 | 0.497 | **0.567** | 0.515 | 0.539 |
| | $p$ | 0.000 | 0.000 | **0.000** | 0.000 | 0.000 |

*Comparison with other precipitation reconstructions in and around our region*

We compared our May–June regional precipitation reconstruction with the reconstructions of Akkemik *et al*. (2005), D'Arrigo and Cullen (2001), and Touchan *et al*. (2003). All the precipitation reconstructions correlate significantly with ours (Table VIIIA). The highest correlation of 0.429 is with the Akkemik *et al*. reconstruction (A05) of March–June precipitation from a tree-ring chronology of modern oaks from a single site within our eastern grid. The correlation is high despite their inclusion of the two months prior to May.

D'Arrigo and Cullen's reconstruction (D01) is of the February–June precipitation for 1628–1980, and is centered on Sivas, Turkey, the easternmost meteorological station in our study region. They used five tree-ring chronologies from across Turkey, including one of the forest chronologies used here from the eastern grid. Their reconstruction also correlates well with our reconstruction, even though it includes the precipitation of February through April as well as May and June (Table VIIIA).

The Touchan *et al*. (2003) reconstruction includes two May–June precipitation reconstructions for southwestern Turkey, one based on the ring widths of juniper alone (*Juniperus excelsa* Bieb.) from 1339 to 1998 (T03–1339) and the other on the tree-ring growth of cedar (*Cedrus libani* A. Rich.), pine (*Pinus brutia* Ten. and *P. nigra* Arn.), and juniper from 1776 to 1998 (T03–1776). The reconstruction is based on the 25–30 E, 35–40 N CRU May–June grid directly to the south of the center of our region. The May–June precipitation reconstruction for 1339–1998 correlates with our reconstruction at 0.193 ($p < 0.001$, $n = 656$), and the 1776–1998 reconstruction correlates at 0.245. ($p < 0.001$, $n = 213$). A visual comparison between the longer of the two reconstructions with ours (Figure 8) shows years of high correlation and years of opposite correlation with occasional 2- to 5-year sequences of opposite extreme growth patterns. A subtraction of their standardized reconstruction from ours clearly indicates periods of similarities, such as the second half of the nineteenth century when it appears that similar precipitation anomalies occurred in the north and south. Periods of sustained opposite precipitation anomalies from north to south, indicated in the opposite values of the two reconstructions from 1476–1479, – the longest severe drought period in southwestern Turkey in the last 600 years (Touchan *et al*., 2003) – are rare.

The correlation coefficients and probability levels in Table VIIIB indicate that the correlations between the oaks and various sets of precipitation anomalies are significantly higher than any correlation of the other reconstructions with the gridded precipitation data. This



DOI: 10.1002/joc

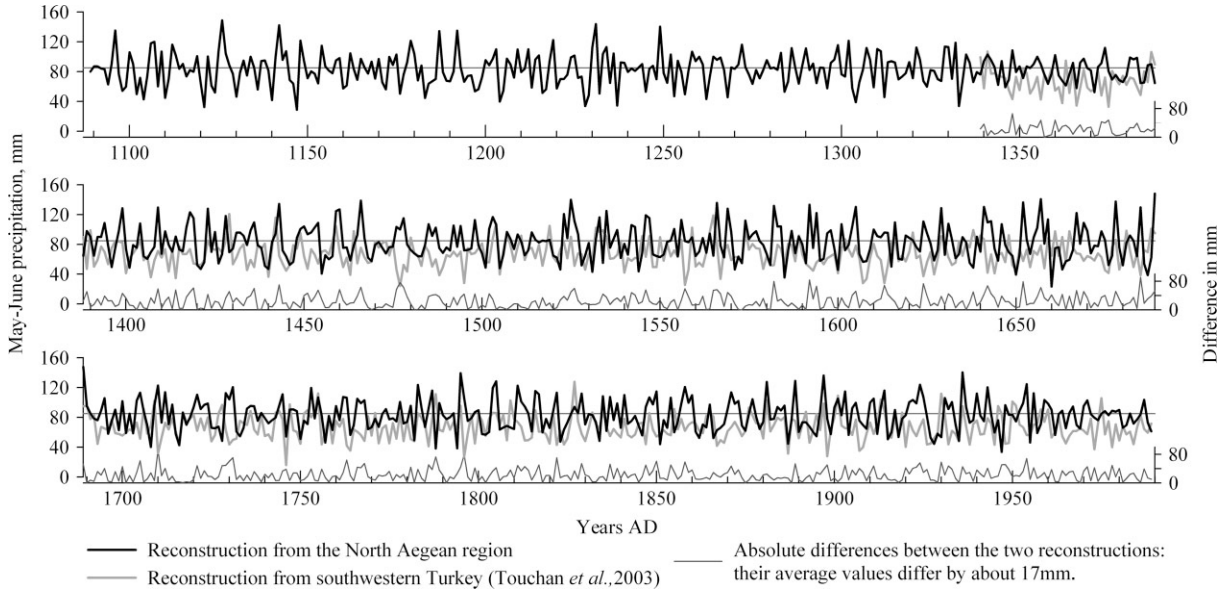


Figure 8. Our reconstructed May–June precipitation values compared to the 1338–1998 May–June reconstruction of Touchan *et al*. (2003). The mean value of the Touchan reconstruction is about 17 mm less than the mean of our reconstruction. Of note are the years when the two reconstructions are very similar (e.g. 1875–1888) and when they are considerably different (e.g. 1475–1480).

comparison indicates that our reconstruction fits in well with the established data sets from this region. It appears that D'Arrigo and Cullen's reconstruction may reflect more of the climate in the southern Turkey region, probably due to their inclusion of tree-ring data from that area. The species used in that and the Touchan *et al*. reconstructions have a higher mean sensitivity and more annual variance in their ring widths than oaks, which may indicate that the methodology used here for optimizing the oaks' response is essential for a good reconstruction from tree-ring data of oak and other ring-porous angiosperms.

## CONCLUSIONS

We have calculated May–June precipitation for the northern Aegean region for A.D. 1089–1989, adding an extension of 234 years to the precipitation reconstruction for the Near East. We have also shown that the high frequency response in these oaks at the southern boundaries of their species' ranges is primarily due to the May–June precipitation, and that the data of samples collected for dendrochronological purposes are secure proxy data for the paleoclimate record of the region. Our tree-ring record also has the potential to be used as proxy data for site-specific May–June temperature changes due to the highly significant negative correlation between precipitation and temperature in the continental subregions where the oaks grow, and extending this chronology to the present will allow us to explore that potential. In continuing research, we have also explored decadal to multidecadal variance in the tree-ring record for possible low-frequency forces and changes in the regional signal over time. Other limiting factors in the spatial and temporal variability of the ring widths are the May North Atlantic Oscillation (NAO) (Griggs *et al*., 2005; Griggs, 2006), plus a strong interrelationship between the winter NAO and the Atlantic Multidecadal Oscillation that affects this region (Touchan *et al*., 2005; Xoplaki, 2002). Further studies of our tree-ring data plus other proxy data sets and tree-ring data from outside the region may provide a critical paleoclimate link between the Atlantic and Indian–Pacific Ocean arenas.

The methodological tests conducted here indicate that the processes of detrending with cubic spline curves and the normalization of the oak ring widths optimized their high-frequency record of the May–June precipitation. However, the necessity of removing the low-frequency signal may indicate that the recent change in growth response is due to anthropogenic influence. The importance of the length of this tree-ring record is that it does show a similar difference between the CSP and LFR chronologies in the late fifteenth century; however, meteorological records are not available to tell us whether this was a response to some other factor besides the May–June precipitation. The differences in the results of the detrending methods must be further examined along with other climate parameters for possible reasons for the low-frequency variation.

The oak tree-ring record of the eastern Mediterranean region is a unique database with a robust record going back into the eleventh century A.D. Further analyses will provide a better assessment of spatial variation in climate, climate change, and the teleconnections of larger-scale climate patterns over the second millennium A.D. Future research also has great potential for clarifying answers to continuing questions about the impact of climate and climate change on human history, and *vice versa*, in one of the earliest civilized areas of the world.



DOI: 10.1002/joc

ACKNOWLEDGEMENTS

Research was funded by NSF grants BCS-0314282 and SBR-9905389, the Malcolm H. Weiner Foundation, and Patrons of the Aegean Dendrochronology Project. Many thanks are due to Ed Cook for his discussion and comments.

REFERENCES

Akkemik Ü, Dağdeviren N, Aras A. 2005. A preliminary reconstruction (A.D. 1635–2000) of spring precipitation using oak tree rings in the western Black Sea region of Turkey. *International Journal of Biometeorology* **49**(5): 297–302 DOI: 10.1007/s00484-004-0249-8.

Atalay I. 2002. *Türkiye'nin Ekolojik Bölgeleri* (Ecoregions of Turkey). Meta Publishers: Baskı, Izmir.

Baillie MGL. 1982. *Tree-ring Dating and Archaeology*. University of Chicago Press: Chicago, IL.

Baillie MGL. 1995. *A Slice Through Time*. B.T. Batsford, Ltd: London.

Baillie MGL, Pilcher JR. 1973. A simple cross-dating program for tree-ring research. *Tree-ring Bulletin* **33**: 7–14.

Blasing TJ, Duvick D. 1984. Reconstruction of precipitation history of North American corn belt using tree rings. *Nature* **307**(12): 143–145.

Cook ER, Jacoby GC. 1979. Evidence for quasi-periodic July drought in the Hudson Valley, New York. *Nature* **282**: 390–392.

Cook ER, Kairiukstis LA (eds). 1990. *Methods of Dendrochronology*. Kluwer Academic Publishers: Dordrecht.

Cook ER, Peters K. 1997. Calculating unbiased tree-ring indices for the study of climatic and environmental change. *Holocene* **7**: 361–370.

Cook ER, Holmes RL. 1999. *Users Manual for Program ARSTAN, February 1999 Edition*. Laboratory of Tree-Ring Research, University of Arizona: Tucson, AZ.

Cook ER, Briffa KR, Meko DM, Graybill D, Funkhouser G. 1995. The 'segment length curse' in long tree-ring chronology development for palaeoclimatic studies. *Holocene* **5**: 229–237.

D'Arrigo R, Cullen HM. 2001. A 350-year (AD 1628–1980) reconstruction of Turkish precipitation. *Dendrochronologia* **19**(2): 169–177.

Davis PH. 1982. *Flora of Turkey and the East Aegean Islands*, Vol. 7. University Press: Edinburgh.

Duvick D, Blasing TJ. 1981. A dendroclimatic reconstruction of annual precipitation amounts in Iowa since 1680. *Water Resources Research* **17**(4): 1173–1189.

Fagan B. 2000. *The Little Ice Age*. Basic Books: New York.

Fritts HC. 1976. *Tree Rings and Climate*. Academic Press: London.

García-Suárez AM. 2005. The influence of climate variables on tree ring widths of different species, PhD dissertation, The Queen's University of Belfast: Northern Ireland.

Gassner G, Christiansen-Weniger F. 1942. Dendroclimatologische Untersuchungen über die Jahresringentwicklung der Kiefern in Anatolien. *Nova Acta Leopoldina: Abhandlungen der Kaiserlich Leopoldinisch-Carolinisch deutschen Akademie der Naturforscher N.F.,* Band 12, No 80.

Gordon GA. 1982. Verification of dendroclimatic reconstructions. In *Climate from Tree Rings*, Hughes MK, Kelly PM, Pilcher JR, LaMarche VC Jr. (eds). Cambridge University Press: Cambridge; 58–61.

Griffiths JF, Driscoll DM. 1982. *Survey of Climatology*. Charles E. Merrill: Columbus, IN.

Griggs CB. 2006. Tale of two: reconstructing climate from tree-rings of the North Aegean, AD 1089–1989, and late Pleistocene to present: dendrochronology in upstate New York, PhD Dissertation, Cornell University: Ithaca.

Griggs CB, DeGaetano AT, Kuniholm PI, Newton MW. 2005. Phase changes of the winter North Atlantic Oscillation recorded in spatial changes in tree-ring patterns of North Aegean oaks, AD 1190–1967. AGU 2005 Fall Meeting Supplement. *EOS Transaction* **52**(86): Abstract PP41C-02.

Grove JM. 2004. *The Little Ice Ages*, *Routledge Studies in Physical Geography and Environment #5*, 2nd edn, Vol. 1. Routledge: London.

Grove JM, Grove AT. 1992. Little Ice Age climates in the Eastern Mediterranean. In *European Climate Reconstructed from Documentary Data: Methods and Results*, Frenzel B (ed.). Palaeoclimate Research, Vol. 7, Special issue, ESF Project: European Palaeoclimate and Man 2. Akademie der Wissenschaften und der Literatur: Mainz.

Hammond N. 2005. Church has Frankish origin. *The London Times*. Times Newspapers Limited: London 4 January 2005: 50.

Huber B, von Jazewitsch W. 1956. Tree-Ring studies of the forestry-botany Institutes of Tharandt and Munich. *Tree-Ring Bulletin* **21**: 28–30.

Hughes MK, Kuniholm PI, Eischeid JK, Garfin G, Griggs CB, Latini C. 2001. Aegean tree-rings signature years explained. *Tree-Ring Research* **57**(1): 67–73.

Hulme M. 1992. A 1951–80 global land precipitation climatology for the evaluation of General Circulation Models. *Climate Dynamics* **7**: 57–72.

Hulme M. 1994. Validation of large-scale precipitation fields in General Circulation Models. In *Global Precipitations and Climate Change*, *NATO ASI Series*, Desbois M, Desalmand F (eds). Springer-Verlag: Berlin; 387–406.

Hulme M, Osborn TJ, Johns TC. 1998. Precipitation sensitivity to global warming: Comparison of observations with HadCM2 simulations. *Geophysical Research Letters* **25**: 3379–3382.

Jones PD. 1988. Large-scale precipitation fluctuations: a comparison of grid-based and areal precipitation estimates. In *Recent Climatic Change, a Regional Approach*, Gregory S (ed.). Belhaven Press: London; 30–40.

Kelly PM, Munro MAR, Hughes MK, Goodess CM. 1989. Climate and signature in West European oaks. *Nature* **340**: 57–60.

Kelly PM, Leuschner HH, Briffa KR, Harris IC. 2002. The climatic interpretation of pan-European signature years in oak ring-width series. *Holocene* **12**(6): 689–694.

Kramer PJ, Kozlowski TT. 1979. *Physiology of Woody Plants*. Academic Press: New York.

Kuniholm PI, Striker CL. 1983. Dendrochronological investigations in the Aegean and neighboring regions, 1977–1982. *Journal of Field Archaeology* **10**: 411–420.

Kuniholm PI, Striker CL. 1987. Dendrochronological investigations in the Aegean and neighboring regions, 1983–1986. *Journal of Field Archaeology* **14**: 385–398.

Kuniholm PI. 1990. Archaeological evidence and non-evidence for climatic change. In *The Earth's Climate and Variability of the Sun Over Recent Millennia*, Runcorn SJ, Pecker J-C (eds). Philosophical Transactions of the Royal Society of London, Series A: **330**(1615): 645–655.

Kuniholm PI. 1994. Long tree-ring chronologies for the eastern Mediterranean. In *Archaeometry 94*, Demirci Ş, Özer AM, Summers GD (eds). TÜBITAK: Ankara; 401–409, Proceedings of the 29th International Symposium on Archaeometry, 9–14 May 1994, Ankara, Turkey.

Kuniholm PI. 2000. Dendrochronologically dated Ottoman monuments. In *A Historical Archaeology of the Ottoman Empire: Breaking New Ground*, Baram U, Carroll L (eds). Kluwer Academic/Plenum: New York; 93–136.

Kuniholm PI. 2004. 2004 Aegean Dendrochronology Project Newsletter, On website http://www.arts.cornell.edu/dendro/2004News/-ADP2004.html.

Lamb HH. 1995. *Climate, History and the Modern World*, 2nd edn. Routledge: London.

Osborn TJ, Briffa KR, Jones PD. 1997. Adjusting variance for sample-size in tree-ring chronologies and other regional mean timeseries. *Dendrochronologia* **15**: 89–99.

Pilcher JR. 1995. Biological consideration in the interpretation of stable isotope ratios in oak tree-rings. *Problems of Stable Isotopes in Tree-rings, Lake Sediments and Peat-bogs As Climatic Evidence for the Holocene*, Paleoclimate Research, Vol 15, Frenzel B (ed.). Akademie der Wissenschaften und der Literatur: Mainz; 157–161.

Pilcher JR, Gray B. 1982. The relationship between oak tree ring growth and climate in Britain. *Journal of Ecology* **70**: 297–304.

Pohl R. 1995. Eine wissensbasierte Erweiterung des Programmsystems Corina zur Dendrochronologie (Unpublished version in English, *CORINA: The Cornell Ring Analysis Program,* available at the ADP laboratory), MS thesis, Technische Universitaet, Berlin.

Schweingruber FH. 1990. *Anatomie europäischer Hölzer – Anatomy of European Woods. Swiss Federal Institute for Forest, Snow, and Landscape Research, Birmensdorf*. Paul Haupt: Berne.

Stahle DW, Hehr JG. 1984. Dendroclimatic relationships of post oak across a precipitation gradient in the southcentral United States. *Annals of the Association of American Geographers* **74**(4): 561–573.

Stahle DW, Cleaveland MK, Dettinger MD, Knowles N. 2001. Ancient blue oaks reveal human impact on San Francisco Bay Salinity. *EOS Transactions* **82**(12): 141–143.

Touchan R, Garfin GM, Meko DM, Funkhouser G, Erkan N, Hughes MK, Wallin BS. 2003. Preliminary reconstructions of

spring precipitation in southwestern Turkey from tree-ring width. *International Journal of Climatology* **23**(2): 157–171, Data archived at the World Data Center for Paleoclimatology, Boulder, Colorado, USA.

Touchan R, Xoplaki E, Funkhouser G, Luterbacher J, Hughes MH, Erkan N, Akkemik U, Stephan J. 2005. Reconstructions of spring/summer precipitation for the Eastern Mediterranean from tree-ring widths and its connection to large-scale atmospheric circulation. *Climate Dynamics* **25**: 75–98.

Wilson RJS, Elling W. 2004. Temporal instability in tree-growth/climate response in the Lower Bavarian Forest region: implications for dendroclimatic reconstruction. *Trees Structure and Function* **18**(1): 19–28.

Wilson RJS, Esper J, Luckman BH. 2004. Utilising historical tree-ring data for dendroclimatology: a case study from the Bavarian Forest, Germany. *Dendrochronologia* **21**(2): 53–68.

Xoplaki E. 2002. Climate variability over the Mediterranean, PhD Dissertation, Universität Bern: Bern.

Zohary M. 1973. *Geobotanical Foundations of the Middle East*, Vol. 1. (Geobotanica selecta Band III). Gustav Fischer: Stuttgart.




DOI: 10.1002/joc